Water/Fat Separation and Off-Resonance Correction for 3T Spiral Breast Imaging

K. L. Granlund[1,2], B. L. Daniel[1], and B. A. Hargreaves[1]

[1]Radiology, Stanford University, Stanford, CA, United States, [2]Electrical Engineering, Stanford University, Stanford, CA, United States

Introduction Spiral imaging has potential to rapidly shorten the acquisition time required for dynamic contrast-enhanced MRI, but has been challenging at 3T because off-resonance leads to unacceptable blurring in the images. Water/fat separation in the presence of B_0 inhomogeneity is especially problematic in breast imaging, where the glandular tissue of interest is surrounded by fat and the geometry causes severe susceptibility-induced field variations. We estimate water and fat images using three-point least-squares estimation and reconstruct the data using the optimal frequency for each voxel [1,2]. We compare three methods of estimating the field map and present the results of multi-frequency reconstruction for 3T spiral breast imaging.

Methods Data were acquired at three different echo times and a least-squares solution was used to find the water and fat images that best fit the three measured signals for a given field map. The least-squares residual is a measure of the error between the measured data and the estimated images. We generated water, fat, and residual images assuming different uniform field maps to build residual functions versus off-resonance frequency (Δf). For the residual res_W, the data were demodulated at the water resonance frequency [2,3]. For res_F, we demodulated the data at the fat resonance frequency. We calculated a cost function, C, as the average of the res_W and res_F functions. A field map was created by finding the Δf that minimizes the residual error for each voxel. This field map is used to reconstruct the fat and water images on a voxel-by-voxel basis using the demodulation frequency that best estimates the measured signals.

We scanned three normal volunteers using a 3D stack-of-spiral acquisition with $TE_{1,2,3}$ = 1.2, 2.0, 2.8ms and TR = 21.4ms on a 3T GE scanner using a four-channel breast coil. We used a 9-interleave spiral, 20x20cm FOV, 1.1x1.1mm^2 resolution in-plane, 32 slices, 3.6mm thickness, a 20º flip angle, linear shims, and a 23-second scan time.

Results Figure 1 shows representative field maps generated by each residual function (a,b,c) alongside an ROI from the fat images (d,e,f). Figure 2 shows the three residual curves for a voxel in a fat region. When demodulating at the water frequency, fat signal from neighboring voxels blurs into the voxel of interest and affects the shape of the residual function. In this case, it results in a broadened minimum and res_W fails to find the optimal Δf.

For comparison, Figure 3 shows the single frequency water (a) and fat (c) reconstructions beside the multi-frequency reconstruction images (b,d) that were generated using the field map in Figure 1c. Severe blurring is visible at the superior edge of the breast in the single frequency images, as indicated by the arrows. The multi-frequency images (c,d) have sharper features, particularly at the water/fat interfaces, shown in the circle.

Discussion This method provides an effective means of simultaneously separating water and fat images and correcting for field inhomogeneity. While the reconstruction is computationally intensive, it is more robust than linear correction methods and can correct for non-linear variations [4]. By demodulating at both the water and fat frequencies, we average out the effects of blurring on the shape of the residual functions. The resulting field map is smoothly varying, as expected, and results in dramatically less blurring in final images.

Conclusion We present a method to correct field inhomogeneities on a voxel-by-voxel basis while separating water and fat images. With robust multi-frequency reconstruction, there is no need for uniform transmit frequency, thus, spatial-spectral excitation can be replaced with conventional non-frequency-selective RF pulses, which allow much shorter TR, TE, and scan times.

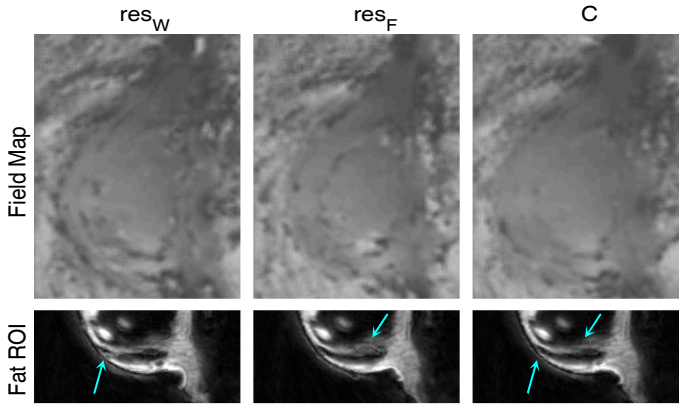

Figure 1: *Estimated field maps and fat images*

The field map based on the cost function (c) is more smoothly varying than the other field maps (a,b) and reveals details in the reconstructed image (f) that were obscured in the images reconstructed based on either res_W (d) or res_F (e), as indicated by the arrows.

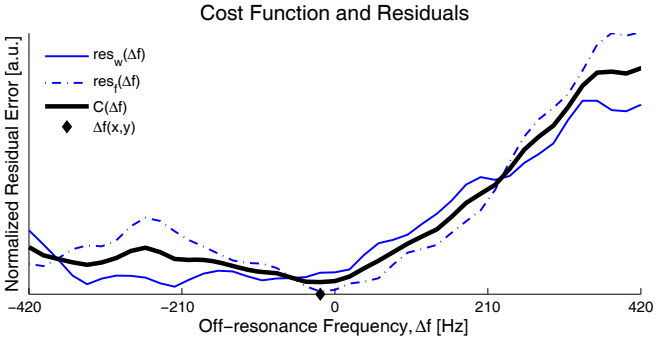

Figure 2: *Representative residuals and cost function*

The residual functions measure the quality of the least-squares estimation; a smaller residual indicates a better fit. The field map is determined by minimizing the residual for each voxel. This figure shows a voxel for which res_W fails to correctly estimate the off-resonance due to the broadened minimum, but the cost function better estimates the field variation, as indicated by the diamond (-20Hz).

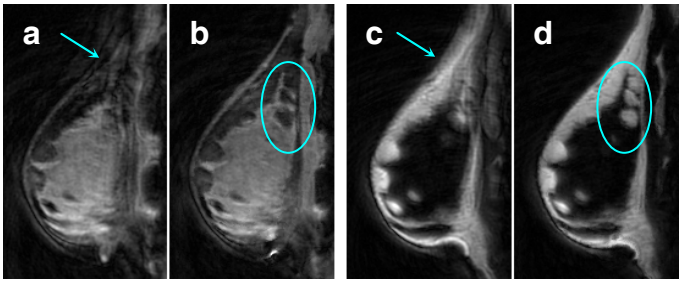

Figure 3: *Breast data for a normal volunteer*

(a) single frequency water image, (b) multi-frequency water image,
(c) single frequency fat image, (d) multi-frequency fat image

The multi-frequency images maintaining proper water/fat separation, yet show better delineation between fat and glandular tissue, as shown in the circled region.

References

[1] Moriguchi, et al., MRM 2003; 50(5):915-24
[2] Gurney, et al., Proc. ISMRM, 2007; 1635.
[3] Reeder, et al., MRM 2004; 51(1):35-45
[4] Irarrazabal, et al., MRM 35(2):278-82 (1996).

Acknowledgements

NIH Grant RR009784
NSF GRFP